A Novel Møller−Plesset Perturbation Based Potential for Determining the Structural and Dynamical Properties of Methane in Silicalite-1: A Molecular Dynamics Study

C. Bussai,[†,‡] S. Fritzsche,[‡] R. Haberlandt,[‡] and S. Hannongbua*[,†]

Department of Chemistry, Faculty of Science, Chulalongkorn University, Bangkok 10330, Thailand, and Department of Molecular Dynamics/Computer Simulations, Institute for Theoretical Physics (ITP), Faculty of Physics and Geoscience, University of Leipzig, Augustusplatz 10−11, 04109 Leipzig, Germany

Received: March 3, 2004; In Final Form: June 8, 2004

A novel silicalite-1/methane potential function model has been developed using quantum chemical calculations at the second-order Møller−Plesset perturbation (MP2) level with the 6-31G* basis sets. Ab initio calculations have been performed at ∼150 methane configurations generated inside the three silicalite-1 segments, namely, $O_{10}Si_{10}H_{20}$, $O_{30}Si_{22}H_{44}$, and $O_{35}Si_{29}H_{58}$. The interaction energies are subsequently fitted to an analytical form. We illustrate characteristics variant between the ab initio fitted potential and the available force-field models. The molecular dynamics simulations, consisting of two units of silicalite-1 cells and eight methane molecules, are performed at various temperatures. The calculated diffusion coefficient 5.53×10^{-9} $m^2 \cdot s^{-1}$ and the heat of adsorption -5.0 kcal·mol^{-1} at room temperature reasonably agree with the previous studies as well as an Arrhenius activation energy of 1.73 kcal·mol^{-1}. The percentages of methane molecules residing in zigzag and straight channels and in the intersection are in good agreement with those reported previously. The methane/methane radial distribution function exhibits the first peak at 6.25 Å. This is in contrast to the previous one observed at ∼4.0 Å. It is, then, demonstrated that the appearance of the peak at 4.0 Å is caused primarily by an imbalance of the methane/methane and silicalite-1/methane pair potentials.

1. Introduction

The proper representation of diffusion in zeolitic material systems is of considerable importance in practice due to their applications in industry and science.[1,2] In particular, ZSM-5 and its dealuminated analogue are widely used in various petrochemical processes, for example, in the conversion of methanol to gasoline.[3] In recent years, molecular simulation techniques, especially molecular dynamics (MD) simulations, have become an essential tool for studying various diffusive guests in zeolites. In most cases, the dynamical results are in good agreement with those obtained from experimental techniques.[4−6] In comparison, structural information is less sufficient.

To the best of our knowledge, the five-center silicalite-1/methane models based on the force-field parametrization by Ruthven et al.[7] and Kiselev et al.[8] were initially available. With a spherical molecule approximation, the "*united atom model*" by Goodbody et al.[9] and by Demontis et al.,[10,11] the methane diffusivities have been investigated using molecular simulations in a rigid and flexible silicalite-1 framework, respectively. Another five-center Lennard-Jones (LJ) model by June et al.[12,13] was calculated according to the Slater−Kirkwood equation and applied in MD simulations. Some structural data were given in these studies via the molecular distributions in the three-dimensional zeolite surface. The authors found out that the small and linear alkanes prefer to reside in the channels, as opposed to the branched alkanes, which prefer to sit in the channel intersections. Grand canonical ensemble Monte Carlo simulations have additionally been performed by the same group, Snurr et al.,[14] in order to predict adsorption isotherms over a range of loadings at various temperatures with the same methane/zeolite model as that used in refs 12 and 13. The obtained adsorption isotherms and heats of adsorption were in good agreement with experiment. Nicholas et al. used the Burkert and Allinger (MM2) model[15] in molecular dynamics simulations to investigate heats of adsorption and self-diffusion coefficients.[16] In the same work, other LJ parameters were extrapolated from ref 17 and proposed by Trouw.[16] The zeolite/alkane models have been improved in computer simulations by comparisons with experimental heats of adsorption and Henry coefficients.[18,19] More recently, Smirnov,[20] Dumont and Bougeard,[21] and Fritzsche et al.[22] have also examined dynamical properties. Due to an increase in computational efficiency to date, a new silicalite-1/methane model has been developed by Engel et al.,[23] as a sum of electrostatic, inductive, dispersive, and repulsive interactions. In addition, simulation results for dynamical properties are frequently compared with those gauged from PFG NMR measurements.[24] However, the structural aspects in terms of pair distribution functions have been reported in depth by Demontis et al.,[10] by Nicholas et al.,[16] and in another attempt by Snurr et al.[14] In all cases, the first peak appeared at about the same position, at ∼4.0 Å.

Due to the fact that all accessible parameters are based on molecular mechanics (MM) parametrization, some doubts may arise when the MM potential is used to represent the dispersive interaction between methane and silicalite-1. For instance, methane/methane LJ parameters were found to cautiously influence methane packing in the specific silicalite-1 structure.[16] The ab initio derived potential reliably demonstrates its ability to describe a proper arrangement of guest molecules inside the pore. We have recently represented a silicalite-1/water interaction by means of an ab initio fitted model that could be fruitfully applied in MD simulations.[25−28]

[†] Chulalongkorn University.
[‡] University of Leipzig.

10.1021/jp0401978 CCC: $27.50
Published on Web 08/10/2004

TABLE 1: Final Optimization Parameters for Atom *i* of Methane Interacting with Atom *j* in Each Channel of the Silicalite-1 Lattice[a]

i	*j*	q_i	q_j	*A* (Å^8 kcal·mol^{-1})	*B* (Å^{12} kcal·mol^{-1})	*C* (Å^{10} kcal·mol^{-1})
C	Si_{sd}	−0.66	0.435	484 120	35 791 283	−7 349 979
C	Si_{st}	−0.66	0.435	2 316 815	283 370 791	−47 973 904
C	O_{sd}	−0.66	−0.87	−113 445	−3 234 971	1 157 607
C	O_{st}	−0.66	−0.87	−185 328	−7 914 489	2 281 723
H	Si_{sd}	0.165	0.435	−67 753	−1 199 457	652 722
H	Si_{st}	0.165	0.435	−141 278	−2 765 365	1 386 542
H	O_{sd}	0.165	−0.87	5704	7620	−13 594
H	O_{st}	0.165	−0.87	−3738	−291 945	94 594

[a] The subscripts sd and st denote sinusoidal (zigzag) and straight channels, respectively. Energies, in kilocalories per mole; distances (r_{ij}'s), in angstroms; and atomic net charges (*q*'s), in atomic units.

Herein, we develop a novel ab initio fitted model used for a molecular dynamics simulation. The simulations are performed at various temperatures, 120, 270, 300, and 350 K. The results are summarized in terms of pair distribution functions, self-diffusion coefficients, heats of adsorption, and activation energies.

2. Calculation Details

2.1. Development of the Intermolecular Pair Potential. Due to the enormous size of the silicalite-1 lattice[29] that consists of 96 silicon and 192 oxygen atoms, the use of quantum chemical calculations to employ the entire unit is undoubtedly impracticable even with the Hartree−Fock method with the small basis set. Therefore, selected rings of $O_{10}Si_{10}H_{20}$, $O_{30}Si_{22}H_{44}$, and $O_{35}Si_{29}H_{58}$ have been taken, respectively, from the zigzag, straight, and intersection channels and have been used to represent the silicalite-1 unit.[30] Experimental geometries of methane[31] and silicalite-1[29] were kept rigid throughout the calculations. To take into account the dispersion interaction which is known to dominate in the methane/silicalite-1 system, the second-order Møller−Plesset perturbation (MP2) level with the extended 6-31G* basis sets, which is shown to be a capable method for the nonpolar covalent molecules,[32] was applied. With regard to our previous work,[30] the basis set superposition error was found to play a slight role on the interaction energy but not on the preferable configuration of the system. Therefore, it was excluded in the present study. The calculations were performed using the G98 program.[33]

The ∼150 configurations of the methane molecule have been generated both in the repulsive and attractive regions inside the three selected rings. Although the methane molecule is spherically symmetric, its orientation was also taken into account. It was moved straight forward to an oxygen and a silicon atom of a fragment, pointing one, two, and three hydrogen atoms to the silicalite-1 surface. The moving step was 0.3 Å starting from the middle of the rings. The ab initio data points, ΔE(m, s), were fitted to an analytical function of the following form:

$$\Delta E(\mathrm{m,\ s}) = \sum_{i}^{5}\sum_{j}^{288}\left\{\frac{A_{ij}^{ab}}{r_{ij}^{8}} + \frac{B_{ij}^{ab}}{r_{ij}^{12}} + \frac{C_{ij}^{ab}}{r_{ij}^{10}} + 332.151\frac{q_i q_j}{r_{ij}}\right\} \quad (1)$$

where 5 and 288 denote the numbers of atoms in a methane molecule (m) and the silicalite-1 (s) unit cell, respectively. The constants A_{ij}, B_{ij}, and C_{ij} are fitting constants, and r_{ij} is the distance between atom *i* of methane and atom *j* of silicalite-1. Also, q_i and q_j are the atomic net charges of atoms *i* and *j* in atomic units, approximated from the population analysis of the isolated molecules in the quantum chemical calculations, where 332.151 is a energy conversion factor (from atomic units to kilocalories per mole). The superscripts *a* and *b* on the fitting parameters have been used to classify atoms in different environmental conditions, that is, in the different channels. The silicalite-1/methane fitting parameters are listed in Table 1.

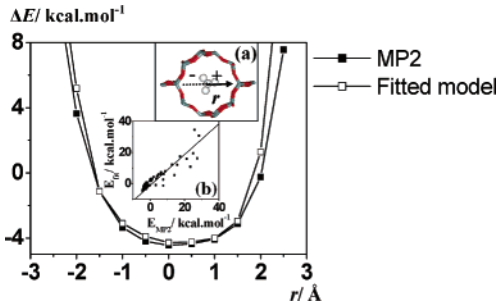

Figure 1. Silicalite-1/methane interaction energies (ΔE values) obtained from the ab initio calculations at the MP2 level with the extended 6-31G* basis sets and from the potential function according to eq 1, where the methane molecule lies along the vector **r** and points a single hydrogen atom to the inner surface of the straight channel, as shown in inset a. All ab initio and fitted data points are also compared in inset b.

2.2. Molecular Dynamics Simulations. The crystallographic silicalite-1 cell[29] has the lattice parameters $a = 20.07$ Å, $b = 19.92$ Å, and $c = 13.42$ Å, characterized by two types of channels with the *Pnma* symmetry group. The simulated silicalite-1 lattice is arranged by $1 \times 1 \times 2$ unit cells with a loading of eight methane molecules or one methane molecule per intersection. The lattice has been assumed to be rigid in this study, as the influence was found not to be very important with regard to the diffusion coefficients[4,22,34] and the structural properties.[10,16] A time step of 1 fs was used to maintain the energy conservation at the temperatures 120, 270, 300, and 350 K. Periodic boundary conditions have been applied. The MP2 methane/methane potential proposed by Rowley et al.[35] and the newly developed silicalite-1/methane potential have been employed. According to refs 36 and 37, the use of Ewald summation can be avoided and a shifted force potential can be applied instead. The evaluation part of each run corresponds to a trajectory length of 10 ns after a 0.5 ps thermalization period.

3. Results and Discussion

3.1. Quality and Characteristics of the Silicalite-1/Methane Potential. Energies, obtained from the quantum chemical calculations and the analytical potential shown in eq 1 with the fitting parameters in Table 1, are visualized in Figure 1. The corresponding configuration, in which the methane molecule points one hydrogen atom to the wall and moves from one side to another side of the wall, along the vector **r** in a straight channel, is given in inset a of Figure 1. The results are plotted in inset b of this figure, where the ab initio and fitted energies of ∼150 data points are compared, especially in the attractive

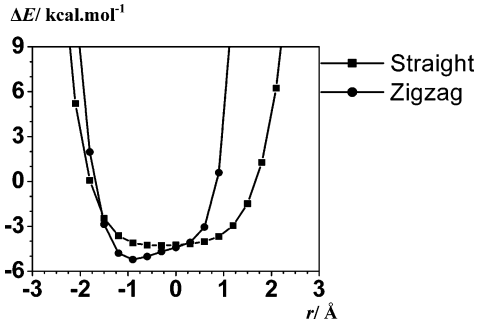

Figure 2. Silicalite-1/methane interaction energies (ΔE values) obtained from the potential function according to eq 1, where the methane molecule in the single-hydrogen configuration moves along the vector **r**, as shown in inset a of Figure 1.

and slightly repulsive regions. The quality of the function is indicated by good agreement between the two sources of energies in the attractive region ($\Delta E < 0$) and satisfactory agreement in the repulsive region.

Concerning an assignment of a negative or positive value to the fitting parameters, it is generally not possible in all cases to make A/r^6 be negative and B/r^{12} be positive, to represent the attractive and repulsive interactions of the pairs, respectively, as well as a 6-12 Lennard-Jones formula. A fit in which the A/r^6 values were separately forced to the van der Waals interaction and the B/r^{12} terms to the repulsion has led to worse agreement with the quantum mechanical results. In these cases, physical meaning of the atomic based pair potentials, 1440 pairs running over $i = 1-5$ and $j = 1-288$ for eq 1, is not achieved. However, the physical meaning as well as the quality of the molecular based methane/silicalite-1 function is its ability in representing ab initio data. An advantage of this approach is that it is a one-to-one correspondence between the predicted (by the potential function) and the observed (by the ab initio calculations) interaction energies. Analogously, as well as for better numerical fitting, the third polynomial term (C/r^{10}) was added and now considered separately. Some examples are those in refs 38 and 39.

The silicalite-1/methane interaction energies when the methane molecule lies in different parts, zigzag and straight segments, have been examined and illustrated in Figure 2. Here, the methane molecule is in the same configuration as that shown in inset a of Figure 1. It reveals that an energy minimum in the zigzag channel of -5.22 kcal·mol^{-1} is slightly lower than -4.28 kcal·mol^{-1}, that in the straight one.

To visualize more detailed characteristics of the ab initio fitted function, the silicalite-1/methane interaction energies in the configuration shown in inset a of Figure 1 have been calculated and compared with those of the available force-field potentials.[8−10,14−18,23] The results are shown in parts a and b of Figure 3 when methane travels along the straight channels starting from the intersection outlet through the adjacent intersection aperture and along the zigzag channel starting from the intersection end, respectively (see the inset). The interaction energies were respectively displayed in parts c and d of Figure 3 when methane moves across the straight and zigzag channels (see the inset).

The plots for all potentials, including ours, display a local minimum at 6.50 Å $\leq l_y \leq$ 7.00 Å along the straight channel (Figure 3a) which indicates favorable residences at the region around the center of the straight section. An additional minimum was detected at $l_y = 2.5$ Å for the Demontis et al. model,[10,11] indicating another local minimum at the intersection. Along the zigzag channel, favorable residences were established in the region of the zigzag interior, 2.10 Å $\leq l_z \leq$ 2.70 Å (Figure 3b).

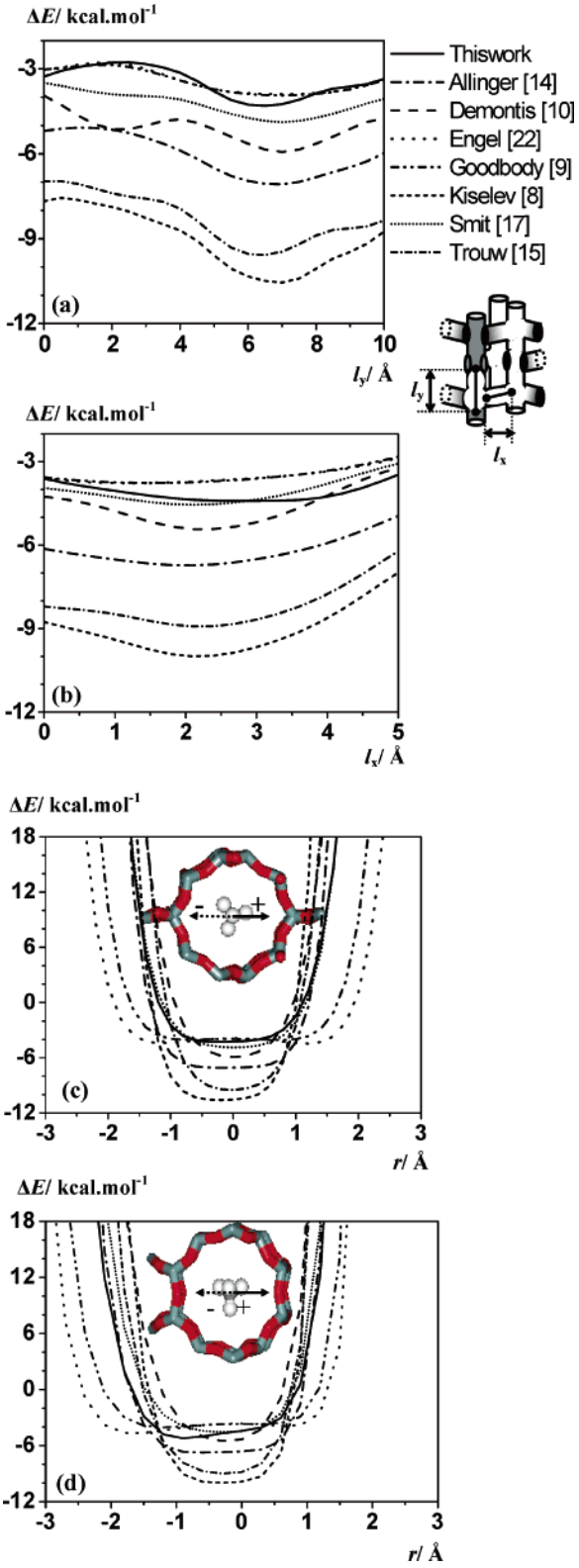

Figure 3. Comparison of the silicalite-1/methane interaction energies (ΔE values) as a function of the distances (l_y, l_x, and r) calculated by various models when methane moves (a and b) along and (c and d) across the straight channel and the zigzag channel, respectively (see text for more details).

Relatively, the optimal energy for all models is observed in the following order: zigzag ~ straight < intersection, validating the prevailing hydrophobicity in the zigzag and straight channels. This is in good agreement with structural data taken from June et al.,[12] where the sitting distributions in the three-dimensional

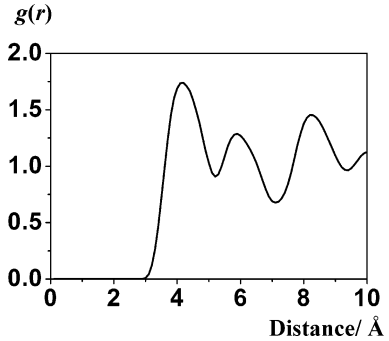

Figure 4. Radial distribution functions [$g(r)$] from oxygen atoms of the silicalite-1 surface to carbon atoms of the methane molecule at 300 K.

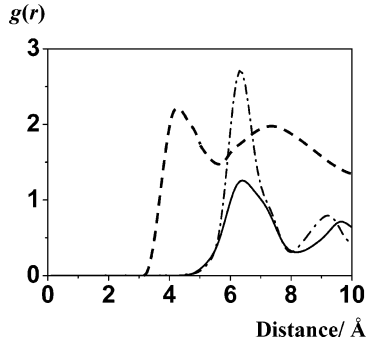

Figure 5. Radial distribution functions [$g(r)$] between the center of mass of the two methane molecules at 300 K: ab initio fitted model, solid line; Nicholas et al.,[15] dashed line. The additional run has been performed using the ab initio fitted model for silicalite-1/methane and Nicholas et al.[15] for methane/methane interactions (dash−dotted line).

contour surface have been evaluated. However, the zigzag channels are also reported as the preferential resident sites for the light alkanes.[6,16]

Figure 3c and d exhibits the accessibilities of how the methane molecule encounters the surface in respect to a potential width; that is, the Engle et al. model[23] shows larger widths, and the Goodbody et al. model[9] allows the methane molecule to move closer to the surface. The asymmetric structure of the curves indicates the model sensitivity. This account could be naively explained due to the configuration asymmetry of the zigzag and straight channels.

In terms of potential depth, the available models yield the energy minimum ranging from -10.50 to -3.50 kcal·mol^{-1}. Although direct experimental data on the methane/silicalite-1 interaction is not available, a minimum of lower than -6 kcal·mol^{-1} is considerably too negative to represent the interaction between a nonpolar molecule such as methane and the hydrophobic channels of silicalite-1. This statement is drawn on the basis of the experimental heat of adsorption between -4.8 and -6.7 kcal·mol^{-1},[40,41] and the calculated values ranged from -4.3 to -5.8 kcal·mol^{-1} [9,10,12,16,24,42] (see section 3.3 for more details). Due to the fact that our results obtained on the basis of ab initio calculations at the MP2 level take into account the dispersion interaction between methane and zeolite and this does not occur in other mechanical methods, we replicate that our detected minimum at -5.22 kcal·mol^{-1} (Figure 3d) is supposed to be the reference minimum for this system.

Note that the diffusion coefficients at various loadings and temperatures obtained from almost all of the available potential functions are in good agreement with those of the experimental observations.[7−16,20−23] This means that this dynamic property is not sensitive either to the depth or the shape of the potential function used. Another reason is due to an error cancellation of the force-field potentials which treat molecular properties as average quantities. These include the use of the united atom approximation for a guest molecule, equivalent treatments of oxygen and silicon atoms in a different environment in the zeolite channels, and implicit treatment of the silicon atom in the silicalite-1 structure, etc. These facts lead consequently to discrepancies of the potential hypersurface in terms of both the depth and the shape as well as the position of the potential minima. Such approximations may not reflect the dynamical properties (due to error cancellation) that are averaged from trajectories of all the channels of silicalite-1 but can lead directly to the deficiency of specific details in the structural data in specific channels.

3.2. Methane Arrangement within the Silicalite-1 Vicinity. The arrangement of methane molecules in the silicalite-1 confines has respectively been monitored in Figures 4 and 5, in terms of the pair distribution functions of silicalite-1/methane and methane/methane. For comparison, the recent existing methane/methane radial distribution function (RDF) has also been given.[16]

3.2.1. Silicalite-1/Methane RDF. The RDF from surface oxygen atoms to methane carbon atoms (Figure 4) displays sharp maxima centered at 4.20, 5.90, and 8.20 Å. Due to the cylinder-like structure with a diameter of ∼8.2 Å of the silicalite-1 channels, the methane molecules that lie under the first peak can be clearly assigned to those moving along the central line, which is defined as the path parallel to the surface and along the center of the tube. This behavior was also detected for the water/silicalite-1 system at sufficiently low loadings.[27,30] Consequently, the other two peaks at 5.90 and 8.20 Å, respectively, allocate to those distances from the carbon atoms of methane to other oxygen atoms of the nearest 10-oxygen-membered ring and of other adjacent rings of the silicalite-1. These established minima are notably in good agreement with those reported previously.[10]

3.2.2. Methane/Methane RDF. Further structural information can be visualized through the RDF between te carbon atoms of the two methane molecules (Figure 5). The plot shows the first sharp peak at 6.25 Å with an apparent minimum at 7.75 Å. In contrast, the existing RDF obtained from molecular dynamics simulations using the Burkert and Allinger[15] model exhibits the first maximum at ∼4.0 Å,[16] (Figure 5, dashed line). The authors explain this finding as the favorable Lennard-Jones interaction between methane molecules.

We deliberate that the favorable methane/methane interaction of ~ -0.10 kcal·mol^{-1} is considerably too weak in comparison to that of silicalite-1/methane of -6.74 kcal·mol^{-1} yielded from the Burkert and Allinger model (see also Figure 3).[16] Therefore, the appearance of the peak at 4.0 Å should be due to methane molecules binding to the surface of the channels. To verify this assumption, a supplementary run has been carried out using the same model for the methane/methane interaction[16] and our ab initio model for the silicalite-1/methane interaction (the optimal energy is -5.22 kcal·mol^{-1}). The obtained C−C RDF is given in Figure 5 (dash−dotted line). The plot demonstrates a first maximum at 6.3 Å, the same position as that obtained from the simulation using our ab initio fitted methane/lattice model. Therefore, a clear conclusion is that the appearance of the peak at 4.0 Å of the C−C RDF is caused primarily by an imbalance of the methane/methane and methane/silicalite-1 pair potentials. In addition, a distance of 6.25 Å of the C−C RDF obtained from our simulation can be assigned to that between the two methane molecules lying in different channels.

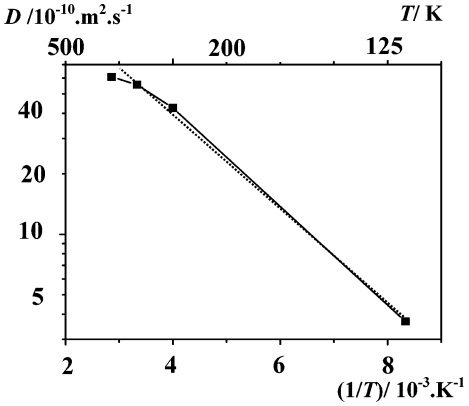

Figure 6. Arrhenius plot of diffusion coefficients (*D*'s) at various temperatures (*T*'s) taken from MD simulations (solid line) and the linear fitted curve (dotted line) for a system containing one methane molecule per intersection of silicalite.

To ascertain more information, methane molecules were classified into three groups regarding the distances to the atoms of the zigzag, straight, and intersection segments. The percentages of time the molecule spent in each channel, zigzag, straight, and intersection, were calculated, which correspondingly amount to 53, 20, and 27%. These ab initio based results agree well with the numbers 56, 29, and 14% reported in ref 16. These data support the previous suggestion of the most favorable resident sites of zigzag channels.

3.3. Diffusion Coefficients, Heats of Adsorption, and Activation Energies. The self-diffusion coefficient has been calculated according to the method described in ref 40. The obtained value 5.53×10^{-9} m^2·s^{-1} approximately agrees with the value $(1.0 \pm 0.2) \times 10^{-8}$ m^2·s^{-1} yielded from the PFG NMR measurements.[24] The activation energy (E_a) can be computed using the Arrhenius equation:

$$D = D_0 \exp(-E_a/RT) \tag{2}$$

where D_0 is a pre-exponential factor. Figure 6 displays the Arrhenius plot, in which ln *D* is a function of temperature. The calculated activation energy 1.73 kcal·mol^{-1} slightly overestimates the previous experimental and theoretical values ranging from 0.5 to 1.2 kcal·mol^{-1}.[10,16,24,43] This may result from a non-Arrhenius behavior of *D* if, for example, the methane molecule experiences barriers of different heights during the diffusion processes. An indication for such barriers is that the plot demonstrates a slightly nonlinear behavior. Nevertheless, the calculated result could be taken as an average energy barrier. The theoretical heat of adsorption ($\langle H \rangle$) can be obtained for low concentrations of guest molecules by the following definition:

$$\langle H \rangle = \langle U \rangle - RT \tag{3}$$

where $\langle U \rangle$ is the average silicalite-1/methane interaction energy. The calculated heat of adsorption −5.0 kcal·mol^{-1} is in good agreement with the experimental data −4.8 and −6.7 kcal·mol^{-1},[40,41] and the calculated values range from −4.3 to −5.8 kcal·mol^{-1}.[9,10,12,16,24,42]

Acknowledgment. Computing facilities provided by the Austrian-Thai Center for Chemical Education and Research at Chulalongkorn University and the Computing Center at Leipzig University are gratefully acknowledged. This work was financially supported by the Thailand Research Fund (TRF). C.B. acknowledges a DAAD-Royal Golden Jubilee Scholarship, Grant No. A/99/16872, and a Royal Golden Jubilee Scholarship, Grant. No. PHD/0090/2541. R.H. and S.F. also thank the DFG (Sonderforschungsbereich 294) for financial support.

References and Notes

(1) Kärger, J.; Ruthven, D. M. *Diffusion in Zeolites and Other Microporous Solids*; Wiley: New York, 1992.
(2) Theodorou, D. N.; Snurr, R. Q.; Bell, A. T. In *Comprehensive Supramolecular Chemistry*; Alberti, G., Bein T., Eds.; Elsevier Science: Oxford, U.K., 1996; Vol. 7, pp 507−548.
(3) Keil, F. J.; Hinderer, J.; Garayhi, A. R. *Catal. Today* **1999**, *50*, 637.
(4) Gergidis, L. N.; Theodorou, D. N.; Jobic, H. *J. Phys. Chem. B* **2000**, *104*, 5541.
(5) Jost, S.; Bär, N. K.; Fritzsche, S.; Haberlandt, R.; Kärger, J. *J. Phys. Chem. B* **1998**, *102*, 6375.
(6) Snurr, R. Q.; Kärger, J. *J. Phys. Chem. B* **1997**, *101*, 6469.
(7) Ruthven, D. M.; Derrah, R. I. *J. Chem. Soc., Faraday Trans. 1* **1972**, *68*, 2332.
(8) Bezus, A. G.; Kiselev, A. V.; Lupatkin, A. A.; Du, P. Q. *J. Chem. Soc., Faraday Trans. 2* **1978**, *74*, 367.
(9) Goodbody, S. J.; Wanatabe, K.; MacGowan, D.; Walton, J. P. R. B.; Quirke, N. *J. Chem. Soc., Faraday. Trans.* **1991**, *87*, 1951.
(10) Demontis, P.; Fois, E. S.; Suffritti, G. B.; Quartieri, S. *J. Phys. Chem.* **1992**, *96*, 1482.
(11) Demontis, P.; Fois, E. S.; Suffritti, G. B.; Quartieri, S. *J. Phys. Chem.* **1990**, *94*, 4329.
(12) June, R. L.; Bell, A. T.; Theodorou, D. N. *J. Phys. Chem.* **1990**, *94*, 8232.
(13) June, R. L.; Bell, A. T.; Theodorou, D. N. *J. Phys. Chem.* **1990**, *94*, 1508.
(14) Snurr, R. Q.; June, R. L.; Bell, A. T.; Theodorou, D. N. *Mol. Simul.* **1991**, *8*, 73.
(15) Burkert, U.; Allinger, N. L. *Molecular Mechanics*; American Chemical Society: Washington, DC, 1982.
(16) Nicholas, J. B.; Trouw, F. R.; Mertz, J. E.; Iton, L. E.; Hopfinger, A. J. *J. Phys. Chem.* **1993**, *97*, 4149.
(17) Allen, M. P.; Tildesley, D. J. *Computer Simulation of Liquids*; Oxford University Press: Oxford, U.K., 1987.
(18) Smit, B. *J. Phys. Chem.* **1995**, *99*, 5597.
(19) Hufton, J. R. *J. Phys. Chem.* **1991**, *95*, 8836.
(20) Smirnov, K. S. *Chem. Phys. Lett.* **1994**, *229*, 250.
(21) Dumont, D.; Bougeard, D. *Zeolites* **1995**, *15*, 650.
(22) Fritzsche, S.; Wolfsberg, M.; Haberlandt, R. *Chem. Phys.* **2003**, *289*, 311.
(23) Ermosshin, V. A.; Engel, V. *J. Phys. Chem. A* **1999**, *103*, 5116.
(24) Caro, J.; Bülow, M.; Schirmer, W.; Kärger, J.; Heink, W.; Pfeifer, H. *J. Chem. Soc., Faraday Trans. 1* **1985**, *81*, 2541.
(25) Bussai, C.; Vasenkov, S.; Liu, H.; Böhlmann, W.; Fritzsche, S.; Hannongbua, S.; Haberlandt, R.; Kärger, J *Appl. Catal., A* **2002**, *232*, 59.
(26) Bussai, C.; Fritzsche, S.; Hannongbua, S.; Haberlandt, R. *Chem. Phys. Lett.* **2002**, *354*, 310.
(27) Bussai, C.; Fritzsche, S.; Haberlandt, R.; Hannongbua, S. *Stud. Surf. Sci. Catal.* **2002**, *142B*, 1979.
(28) Bussai, C.; Fritzsche, S.; Haberlandt, R.; Hannongbua, S. Submitted for publication.
(29) Olson, D. H.; Kokotailo, G. T.; Lawton, S. L.; Meier, W. M. *J. Phys. Chem.* **1981**, *85*, 2238.
(30) Bussai, C.; Hannongbua, S.; Haberlandt, R. *J. Phys. Chem. B* **2001**, *105*, 3409.
(31) Roder, P. M. *J. Phys. Chem.* **1990**, *94*, 6080.
(32) Elstner, M.; Hobza, P.; Frauenheim, T.; Suhai, S.; Kaxiras, E. *J. Chem. Phys.* **2001**, *114*, 5149.
(33) Frisch, M. J.; Trucks, G. W.; Schlegel, H. B.; Scuseria, G. E.; Robb, M. A.; Cheeseman, J. R.; Zakrzewski, V. G.; Montgomery, J. A.; Stratmann, R. E.; Burant, J. C.; Dapprich, S.; Millam, J. M.; Daniels, A. D.; Kudin, K. N.; Strain, M. C.; Farkas, O.; Tomasi, J.; Barone, V.; Cossi, M.; Cammi, R.; Mennucci, B.; Pomelli, C.; Adamo, C.; Clifford, S.; Ochterski, J.; Petersson, G. A.; Ayala, P. Y.; Cui, Q.; Morokuma, K.; Malick, D. K.; Rabuck, A. D.; Raghavachari, K.; Foresman, J. B.; Cioslowki, J.; Ortiz, J. V.; Stefanov, B. B.; Liu, G.; Liashenko, A.; Piskorz, P.; Komaromi, I.; Gomperts, R.; Martin, R. L.; Fox, D. J.; Keith, T.; Al-Laham, M. A.; Peng, C. Y.; Nanayakkara, A.; Gonzalez, C.; Challacombe, M.; Gill, P. M. W.; Johnson, B. G.; Chen, W.; Wong, M. W.; L Andres, J.; Head-Gordon, M.; Replogle, E. S.; Pople, J. A. *Gaussian 98*, revision A; Gaussian, Inc.: Pittsburgh: PA, 1998.
(34) Skoulidas, A. I.; Sholl, D. S. *J. Phys. Chem. B* **2002**, *106*, 5058.
(35) Rowley, R. L.; Pakken, T. *J. Chem. Phys.* **1999**, *110*, 3368.
(36) Wolf, D.; Keblinski, P.; Phillpot, S. R.; Eggebrecht, J. *J. Chem. Phys.* **1999**, *110*, 8254.
(37) Dufner, H.; Kast, S. M.; Brickmann, J.; Schlenkrich, M. *J. Comput. Chem.* **1997**, *18*, 660.

(38) Jorgensen, W. L.; Cournoyer, M. E. *J. Am. Chem. Soc.* **1978**, *100*, 4942.
(39) Karlström, G.; Linse, P.; Wallqvist, A.; Jönsson, B. *J. Am. Chem. Soc.* **1983**, *105*, 3777.
(40) Fritzsche, S.; Haberlandt, R.; Kärger, J.; Pfeiffer, H.; Wolfsberg, M.; Heinzinger, K. *Chem. Phys. Lett.* **1992**, *198*, 283.
(41) Jobic, H.; Beé, M.; Kearley, G. J. *Zeolites* **1989**, *9*, 312.
(42) Papp, H.; Hinsen, W.; Do, N. T.; Bearns, M. *Thermochim. Acta* **1984**, *82*, 137.
(43) Vigné-Maeder, F.; Auroux, A. *J. Phys. Chem.* **1990**, *94*, 316.